Transmembrane Helix Structure, Dynamics, and Interactions: Multi-Nanosecond Molecular Dynamics Simulations

Liyang Shen, Donna Bassolino, and Terry Stouch
Department of Macromolecular Modeling, Bristol-Myers Squibb Research Institute, Princeton, New Jersey 08543-4000 USA

ABSTRACT To probe the fundamentals of membrane/protein interactions, all-atom multi-nanosecond molecular dynamics simulations were conducted on a single transmembrane poly(32)alanine helix in a fully solvated dimyristoyphosphatidylcholine (DMPC) bilayer. The central 12 residues, which interact only with the lipid hydrocarbon chains, maintained a very stable helical structure. Helical regions extended beyond these central 12 residues, but interactions with the lipid fatty-acyl ester linkages, the lipid headgroups, and water molecules made the helix less stable in this region. The C and N termini, exposed largely to water, existed as random coils. As a whole, the helix tilted substantially, from perpendicular to the bilayer plane (0°) to a 30° tilt. The helix experienced a bend at its middle, and the two halves of the helix at times assumed substantially different tilts. Frequent hydrogen bonding, of up to 0.7 ns in duration, occurred between peptide and lipid molecules. This resulted in correlated translational diffusion between the helix and a few lipid molecules. Because of the large variation in lipid conformation, the lipid environment of the peptide was not well defined in terms of "annular" lipids and on average consisted of 18 lipid molecules. When compared with a "neat" bilayer without peptide, no significant difference was seen in the bilayer thickness, lipid conformations or diffusion, or headgroup orientation. However, the lipid hydrocarbon chain order parameters showed a significant decrease in order, especially in those methylene groups closest to the headgroup.

INTRODUCTION

The importance of transmembrane proteins (TM, TMP) cannot be disputed, nor can the difficulty of their experimental investigation. Only recently have spectroscopic approaches such as NMR, infrared (IR), circular dichroism (CD) (Zhang et al., 1995a,b; Hu et al., 1995; de Jongh et al., 1994; Killian et al., 1990; Vogt et al., 1994; Killian, 1992; Challou et al., 1994; Cross and Opella, 1994; Goormaghtigh and Ruysschaert, 1990; Seelig and Seelig, 1974, 1977), x-ray crystallography and neutron scattering (Wiener et al., 1991; Wiener and White, 1991, 1992; White and Wimley, 1994; Weiss and Schulz, 1992; Yeates et al., 1988), DSC (Zhang et al., 1995b; Seelig et al., 1993), and other techniques started to yield definitive insight into TMP structure, dynamics, functions, and relationships to other membrane components. However, despite these latest advances, a detailed atomic-level understanding of these important macromolecules is still elusive.

As computational approaches have matured, they have become routine tools in the study of biological molecules (Brooks et al., 1988; McCammon and Harvey, 1987). However, explicit studies of TMP within membranes is a daunting computational task because of their size, time scales of motions, and long-range electrostatic interactions.

A number of computational studies have employed elegant approximations to reduce the degrees of freedom and hence the computational intensity of such studies. These include investigations into hydrophobic mismatch (Sperotto and Mouritsen, 1991), the existence of lipid annuluses (Edholm and Johansson, 1987), peptide conformations at interfaces (Guba et al., 1994), ordering/disordering of lipids due to proteins (Scott, 1986), and even such impressive phenomena as protein insertion and folding (Milik and Skolnick, 1993) and the effects of adsorbed macromolecules (Pink et al., 1993). Despite the insight gained by this work, there remain questions regarding the level of importance of the missing degrees of freedom for understanding the many different properties and interactions of these proteins. Some studies have employed greater levels of detail, but necessarily could not span large time scales (Edholm and Johansson, 1987).

Furthermore, many studies have employed approximations such as "united atoms" and short-range (8–10 Å) truncation of electrostatic forces, which, although so widespread as to be a standard, have recently been shown to have significant effects on calculated dynamical properties (Muller-Plathe et al., 1992; Bareman et al., 1993; Pant and Boyd, 1993; Yoon et al., 1993; Alper et al., 1993a; Auffinger et al., 1996; Loncharich and Brooks, 1989; Smith and Pettitt, 1991; Kitson et al., 1993; Cheatham et al., 1995; Schreiber and Steinhauser, 1992). Primarily as a result of increased computer power, simulation of biomembranes has become more detailed and longer, and has dealt with increasingly complex phenomena (Stouch and Bassolino, 1996; Bassolino-Klimas et al., 1995; Alper et al., 1993b; Bassolino et al., 1993; Stouch, 1993; Pastor et al., 1991; Damodaran et al., 1992; Egberts and Berendsen, 1988; Xing and Scott, 1989; Shinoda et al., 1995; Heller et al., 1993; Venable et al., 1993; Huang et al., 1994; Essex et al., 1994; Wilson and Pohorille, 1994; Raghaven et al., 1992; Chiu et al., 1995; Woolf and Roux, 1996).

Received for publication 31 May 1996 and in final form 27 March 1997.

Address reprint requests to Dr. Terry Stouch, Department of Macromolecular Modeling, Bristol-Myers Squibb Research Institute, P.O. Box 4000, Princeton, NJ 08543-4000. Tel.: 609-252-5442; Fax: 609-252-6030; E-mail: stouch@bms.com.

0006-3495/97/07/03/18 $2.00

Recently we have reported on a number of multi-nanosecond simulations of phospholipid bilayers that reproduced well many experimental observables, and were stable and well converged (Stouch and Bassolino, 1996; Stouch, 1993; Stouch et al., 1994; Alper et al., 1993a,b; Bassolino et al., 1993; Bassolino-Klimas et al., 1995). These included investigations into bilayer structure and dynamics, the effects of electrostatic truncation, the ordering of solvating water, and the movement and free energy of partitioning of small molecules.

Here we report on studies that extend the previous work by incorporation of a transmembrane protein. The understanding of the properties of even isolated, idealized, single, homogeneous α-helices in vacuum or simple solvents has been the justifiable object of considerable study (Pleiss and Jahnig, 1991, 1992; Edholm and Johansson, 1987; Van Buuren and Berendsen, 1993; Daggett and Levitt, 1992; Perahia et al., 1990; Kovacs et al., 1995). The introduction of such a construct into the heterogeneous, variable, and relatively disordered environment of a solvated lipid bilayer very substantially complicates the study of even such a simple object. For this reason, this study into TMP concerns only a single homogeneous TM helix of alanine. Specifically avoided were the more complex localization or signal sequences or commonly seen charged or aromatic residues at the "headgroup" region, which will be the focus of future studies.

Our ultimate goal is to understand the function of those more interesting sequences and interactions. Yet we currently have no benchmark or standard with which to make comparison. Furthermore, although the concept of membrane regions such as the "hydrophobic core" or the "headgroup" are intuitively simple, much of the membrane is in a state of "tumultuous chemical heterogeneity" (Wiener and White, 1992; White and Wimley, 1994), and at the atomic level these regions are not so simple to define. The development of such a standard using the simplest of the hydrophobic helix-forming peptides is the intent of this study. Here we attempt to understand, in detail, the influence of the membrane environment on this peptide structure and dynamics. In subsequent studies, by comparison to this work, we will probe the effects of the presence of other amino acids and more complex sequences.

METHODOLOGY

The initial model was built from a snapshot of a well-equilibrated (over 4 ns of production), fully hydrated (29 water molecules per lipid molecule) dimyristoyphosphatidylcholine (DMPC) bilayer in the L_α phase (Stouch, 1993). Recently there has been substantial discussion regarding the correct surface area in the bilayer plane occupied per phosphocholine lipid molecule (Nagle et al., 1996; Nagle, 1993; Feller et al., 1995; Chiu, 1995; Tu et al., 1996; Tieleman and Berendsen, 1996; Feller and Pastor, 1996). Experiment has placed this value anywhere from 58 to 72 $Å^2$, a range also duplicated by constant pressure or constant surface tension simulations. Using a model that assumes little "back-bending" of lipid hydrocarbon chains (conformations such that the hydrocarbon chains bend back toward the water layer), Nagle has determined this value to be 62 $Å^2$, later revising the estimate upward to 62.9 $Å^2$. Should such back-bending be found to be significant, this estimate would necessarily be adjusted upward. For this study we started from a bilayer with a value of 66 $Å^2$, close to Nagle's value (Nagle, personal communication). In our own laboratory, we find that surface area values from ~64 to 66 $Å^2$ are equally able to reproduce the order parameters derived from NMR quadrapolor splittings within the error of experiment and simulation (T. Stouch, unpublished results).

Because little is known about the surface area of a peptide helix in a bilayer, we chose a surface area that could be accommodated by an idealized α-helix (100 $Å^2$) plus the factor for thermal expansion seen for lipid molecules (expanding from a value in the crystalline state of 40 $Å^2$ to ~60–70 $Å^2$ in the liquid crystalline state) to provide a surface area for the peptide of roughly about that of two lipid molecules, 133 $Å^2$. This value for the peptide, coupled with a reasonable estimate of the surface areas of the lipids of 66 $Å^2$, provides an overall surface area that is well within the surface area estimates for lipid molecules derived either from experiment or from simulation. In light of Nagle's values, one might question if this is slightly too large. If this were so, one might expect the lateral pressure of the system to be negative. In fact, the average lateral pressure of the system was positive, ~100 bar (86 ± 600), a value typical for biomolecular simulations.

To accommodate the peptide, two lipid molecules were removed from each monolayer to form a rough cylindrical region. It has been well established that in this phase, lipid molecules have a wide range of conformations and are quite entangled (Stouch, 1993; Pastor et al., 1991; Egberts and Berendsen, 1988). Consequently, even removal of these four lipid molecules did not create an empty void. To clear a volume that could easily accommodate a transmembrane helix, a weak cylindrical repulsive force was centered in the vacated region during subsequent energy minimization (steepest descents, 2000 iterations) and 20 ps of low temperature molecular dynamics simulation (as described below). This gently cleared a volume of water and, primarily by torsional isomerization, lipid hydrocarbon chains. The repulsive force was removed and was not used after this time. A 32-residue polyalanine α-helix at idealized α-helical backbone torsion angles was inserted in the resulting volume. The system in total then consisted of a 32-mer of polyalanine, 16 lipid molecules in each monolayer for a total of 32 lipid molecules, 481 water molecules per monolayer in a two-dimensional box periodic in the plane of the bilayer of dimensions 34.5 × 34.5 Å. A weak restraining force as described previously (Stouch, 1993; Alper et al., 1993a) was used to maintain the third dimension at 60.6 Å. The system was energy minimized (steepest descent, 2000 iterations) to remove any protein overlap with water or

lipids and to reduce the thermal energy remaining from the MD simulation. It was then gradually rethermalized (50 K increments for 1000 steps at each temperature) to the final production temperature of 320 K, 23 K above the gel-to-L_α phase transition for hydrated DMPC. Equilibration was continued for an additional 100 ps, and these data were discarded. Production runs followed for an additional 1.66 ns, during which the trajectory was saved every 100 fs. An additional set of data was saved every 5 ps, which was used for much of the analysis.

For comparison with the membrane simulation as well as with the literature concerning helix dynamics and stability and as a further verification of the protein force field, a separate simulation of a single 32-residue polyalanine in vacuum was run for 3 ns under similar conditions.

As described previously, the force fields for the lipid molecules (Stouch et al., 1991; Stouch, 1993) and water (Lau et al., 1994) were extensions of the consistent valence force field (Hagler et al., 1979a,b; Dauber-Osguthorpe et al., 1988), and the consistent valence force field was used for the protein. The nonbonded interactions (Coulomb and Lennard-Jones terms) between the zwitterionic headgroups (choline and phosphate moieties) of the lipid molecules and everything else were evaluated to 16 Å. All other interactions were evaluated to 10 Å.

An in-house, substantially modified version of the Discover version 2.6 program was used (Molecular Simulations, San Diego, CA). The Verlet algorithm was used for MD integration (1.0-fs time step), and the temperature was maintained by coupling water and lipids to separate external baths (Berendsen et al., 1984). All simulations were run on a Cray Y-MP/2-32. Some of the analysis was done using in-house software; however, most of it was performed using Beta-test versions of the Decipher program (Molecular Simulations).

RESULTS

Fig. 1 *a* shows the initial starting configuration, and Fig. 1 *b* displays a series of snapshots of the protein at particular times over the 1.66-ns trajectory. As mentioned, initially the entire peptide was built as an "ideal" α-helix perpendicular to the plane of the bilayer.

During the 100-ps heating and equilibration, the N and C termini (Ala^1-Ala^{11} and Ala^{25}-Ala^{32}), which were exposed to the lipid headgroup region and, in particular, the water region, denatured, and the peptide helix tilted ~10°. During the remainder of the simulation, the termini assumed a number of distinctively different coiled conformations, and the tilt of the helical region varied dynamically. The middle segment of the peptide, Ala^{12}-Ala^{24}, located in the lipid hydrocarbon chain region, maintained a stable, mostly α-helical structure.

The molecular dynamics of even this small peptide in the lipid bilayer has many facets. To clearly present the results and detailed analysis of our simulation, we divide the results into four parts. First we investigate the dynamic structure of the peptide itself. Second, the peptide-lipid interactions and the surrounding environment structures are discussed. Third, the bulk properties of the membrane are presented. Finally, we examine the behavior of lipid molecules.

Transmembrane peptide properties

α-Helicity

Fig. 2, *a* and *c*, shows the statistics of the ϕ and ψ angles for each residue averaged over the entire production trajectory. The segment of the peptide located in the hydrocarbon chain region, Ala^{12}-Ala^{24}, was a very stable α-helix, as evidenced by the average ϕ, ψ values of −70.0° and −39.7° (versus ideal values of −100 to −40 and −60 to −20) and small standard deviations (which were quite comparable in magnitude to those found in simulations of other systems and employing other force fields (Miick et al., 1993; Van Buuren and Berendsen, 1993; Daggett and Levitt, 1992; Daggett et al., 1991)). The stability is further reflected by the high fraction of time that these torsions reside at the helical values (Fig. 2, *b* and *d*). Just beyond this "core" helical region were the sequences containing residues 8–12 and 25–28. Although their average ϕ and ψ values indicate that they were predominantly helical, the standard deviations are larger and the α-helical residence times are lower, showing less stable α-helical structures. Beyond these stretches, the most terminal segments of the peptide were exposed to lipid headgroups and to water and have statistics substantially different from those of an ideal α-helical structure. Although most of the ϕ angles were within the α-helical range, the ψ angles were well beyond the region. The standard deviations of these values were far larger than those in the rest of the peptide, and residence times in the α-helical conformation were low. The statistics reflected variable coiled structures.

To further probe the α-helicity of the peptide, the characteristic α-helical O(i) to H-N(i + 4) hydrogen bond distance statistics are displayed in Fig. 3 *a*, and the residence time of these distances within 3.0 Å is shown in Fig. 3 *b*. Steady H bonds existed in the "core" middle segment (residues 12–24) over 75% of the time, with an average H-bond distance of 2.6 Å and standard deviations typically less than 0.7 Å. (The large value of these distances will be discussed presently.) Although α-helical-like, intrapeptide H bonding occurred for some residue pairs within the terminal segments, this was completely absent for most residue pairs in the N- and C-terminal 4–8 residues.

Although the central segment displayed stable α-helical structure, it was not inflexible. This is demonstrated by the backbone root-mean-square deviation (rmsd) of each configuration from the starting (postequilibrated) configuration (backbone of Ala^{12}-Ala^{26} maximally superimposed). Before 0.9 ns the rmsd was ~0.7 Å, but at ~0.9 ns it increased abruptly to ~1.9 Å and remained at that value for the remainder of the simulation. This change coincided with a

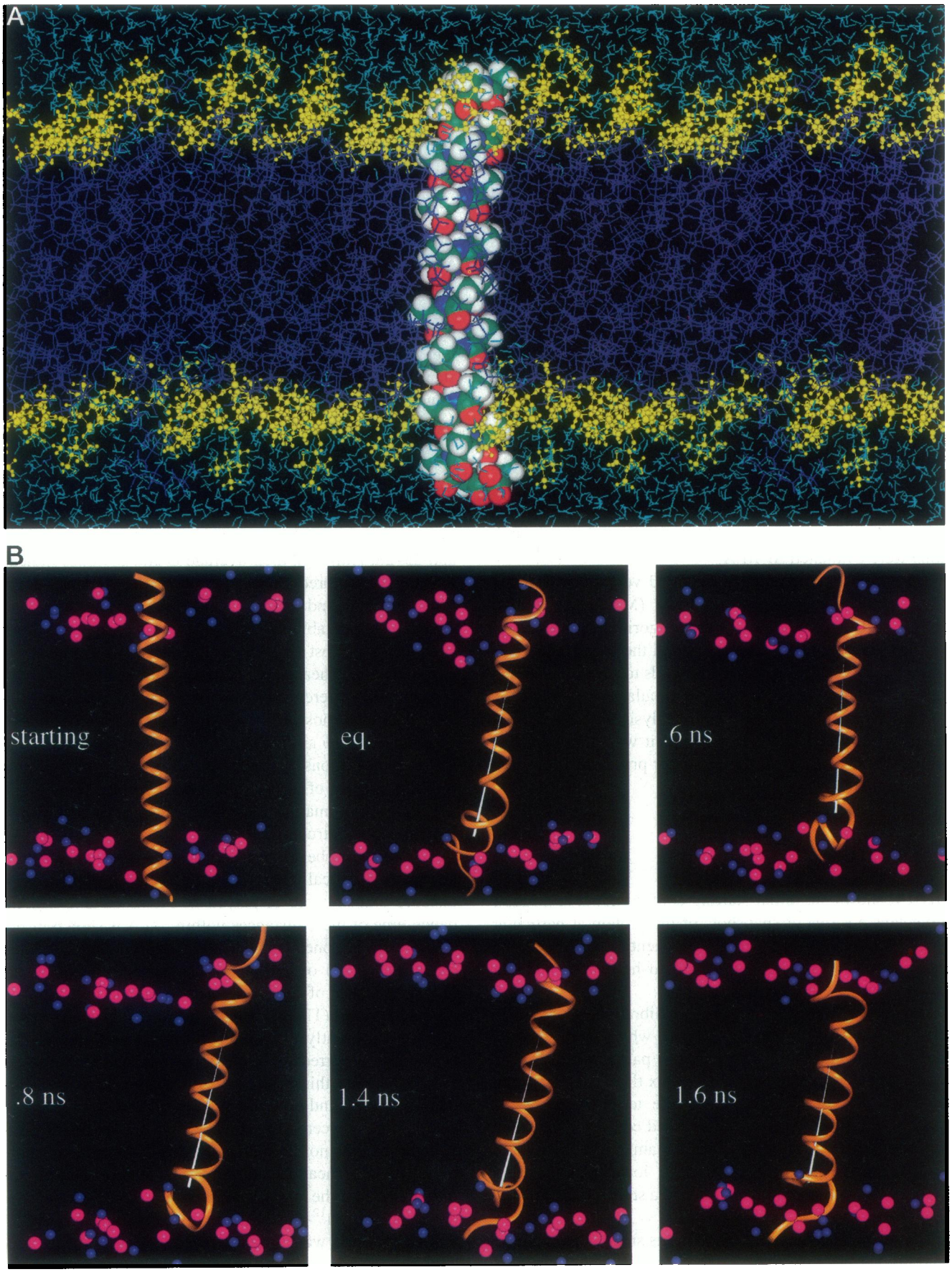
A
B
starting
eq.
.6 ns
.8 ns
1.4 ns
1.6 ns

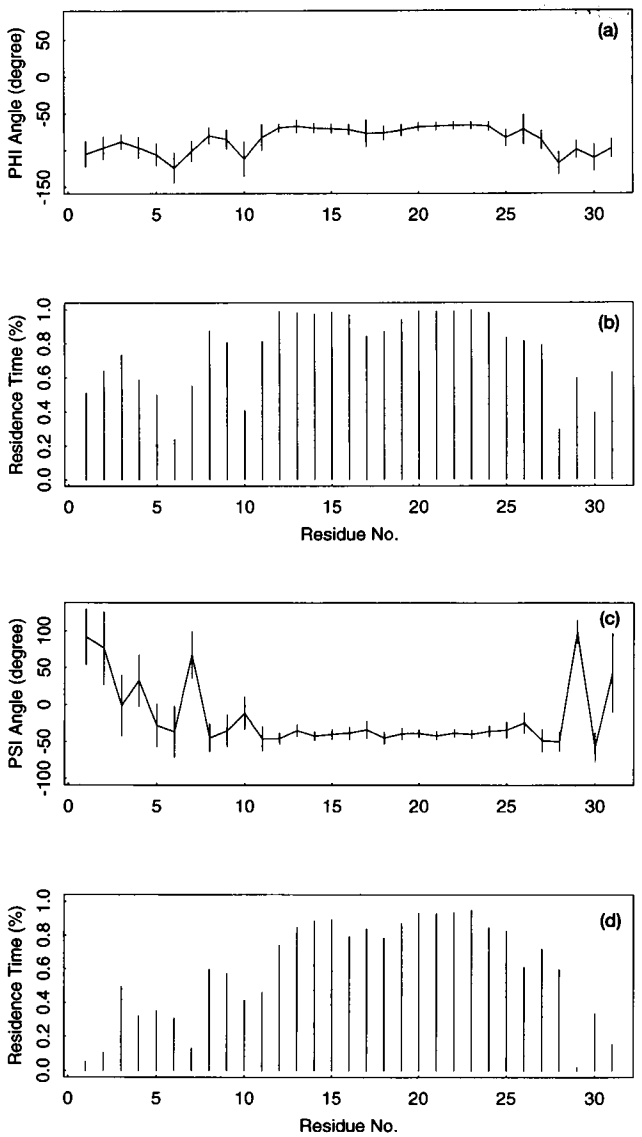

FIGURE 2 (*a*) The average PHI angle (ϕ) of the $(Ala)_{32}$ peptide in the DMPC lipid bilayer. (*b*) The residence times (%) of time that ϕ appeared in the helical range of [−100°,−40°]. (*c*) The average PSI angle (ϕ). (*d*) The residence time (range of [−60°,−20°]).

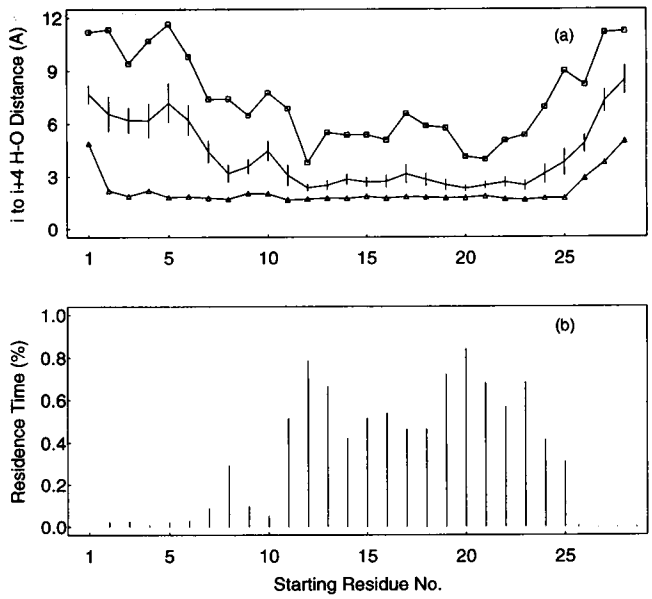

FIGURE 3 (*a*) The values of $i \rightarrow i + 4$ H-bond distances (i.e., from N-H(i) to C═O(i + 4)) for the $(Ala)_{32}$ peptide in the DMPC lipid bilayer. The solid line with bars stands for the average value and the standard deviation, and the line with open squares and the line with triangles give the maximum and minimum distances observed over the 1.66-ns simulation time. (*b*) The residence time (%) of the $i \rightarrow i + 4$ H-bonding, with a distance of less than 2.6 Å. Percentage peptide structures at a given time versus the structure at the initial simulation time

slight shortening of the helix and a corresponding increase in the cross section, as will be discussed. The changes to the core region were well contained relative to the changes for the entire peptide, however. The rmsd for the entire peptide backbone, including the regions in the water and headgroup regions, increased much more substantially, achieving a value of ~3.8 Å early in the simulation, fluctuating substantially, and eventually attaining a value of 4.3 Å. These large values and fluctuations were due to large conformational changes in the coiled states of the two most terminal segments.

For residues Ala^{12}-Ala^{26}, quantification of the cross-sectional radius (by taking the average of the distances of the C_α atoms to the helical axis) versus time showed a step change from 2.4 Å to 2.6 Å at ~0.95 ns, corresponding to the shift in rmsd. The length of this transmembrane region, as well as the terminal stretches, was quantified by the distances between the terminal C_α atoms of each region, i.e., $C_\alpha 12$ to $C_\alpha 26$, $C_\alpha 1$ to $C_\alpha 11$, and $C_\alpha 27$-$C_\alpha 32$. The length of the helical segment oscillated between 20 Å and 23 Å with a small amplitude of only a few angstroms. At ~0.95 ns, a small decrease occurred, from a mean value of 21.9 Å to 20.6 Å, resulting in the overall shortening of 1.3 Å, mentioned above. Despite these changes, the mean length per residue was 1.5 Å (SD 0.05, range 1.4–1.7 Å), well within α-helical parameters. The corresponding profiles for the terminal segments showed large changes, reflecting their changing configurations.

These changes in the central helix, as well as the large average values for the $i \rightarrow i + 4$ hydrogen bonds, are due to shifts between different helical forms. Such shifts are seen widely in MD simulations of helices (Smythe et al.,

FIGURE 1 (*a*) A structure of helical $(Ala)_{32}$ peptide in a fully-hydrated DMPC bilayer. (*b*) A set of snapshots of the $(Ala)_{32}$-peptide (*ribbon*) in the DMPC lipid bilayer at different simulation times. For the lipid molecules, we only show here their phosphorus atoms (*magenta CPK*) and the nitrogen atoms (*blue CPK*). An ideal α-helix was built for the $(Ala)_{32}$ peptide as a starting structure. The periodic boundary images used in the simulation are shown.

1993; Van Buuren and Berendsen, 1993) and are suggested by experiment (Zhang et al., 1995a). Frequently, individual residues or short stretches of two to six residues interconverted between the α- and either the 3_{10} or π-helical types. Statistics of the distances of the respective characteristic $i \rightarrow i + 3$ and $i \rightarrow i + 5$ hydrogen bond patterns for these helical types are shown in Figs. 4 and 5. As indicated by the residence times for the individual residues, overall the alternate forms were not common. However, as seen repeatedly elsewhere (Miick et al., 1993; Smythe et al., 1993; Pleiss and Jahnig, 1991; Van Buuren and Berendsen, 1993; Daggett and Levitt, 1992; Zhang et al., 1995a), the entire helical region (residues Ala^{12}-Ala^{26}) assumed a 3_{10} form ~10% of the time. At isolated regions (the helix center and ends) the π form was sampled from 10% to as much as 60% of the time. That at any one time only portions of the helix were in these alternate forms is reflected by the overall helix length and radius. The length of the 15-residue "core" helix never approached the 30-Å length of an ideal 3_{10} helix or the 16.5-Å length of an ideal π helix. Rather, as noted above, it fluctuated about the 22 Å length expected of the α form. Furthermore, although the radius of the helix approached the 2.8 Å value for a π form, it never became as small as the 1.9 Å of the 3_{10} form.

Translation and diffusion

The peptide showed substantial translational movement over the simulation, as shown by a plot of the center of mass of Ala^{12}-Ala^{26} versus time (Fig. 6 *a*). It moved substantially in all three directions, oscillating in place over short times and exhibiting a net movement over longer times. The range of positions was 5.1 Å, 6.5 Å, 12.4 Å in x, y, and z, where x and z define the bilayer plane. Note that the peptide showed greater lateral movement (within the bilayer plane) than transverse movement (normal to the plane). The results imply that lateral movement was easier than transverse movement. This is further substantiated by the fact that diffusion perpendicular to the bilayer plane is about one-third that within the plane (Fig. 6 *b*). The two-dimensional lateral diffusion constant (diffusion within the bilayer plane) calculated from the mean square displacement (MSD) of the center of mass of Ala^{12}-Ala^{26} (Fig. 6 *b*) was $0.97 \pm 1.0 \times 10^{-6}$ cm^2/s.

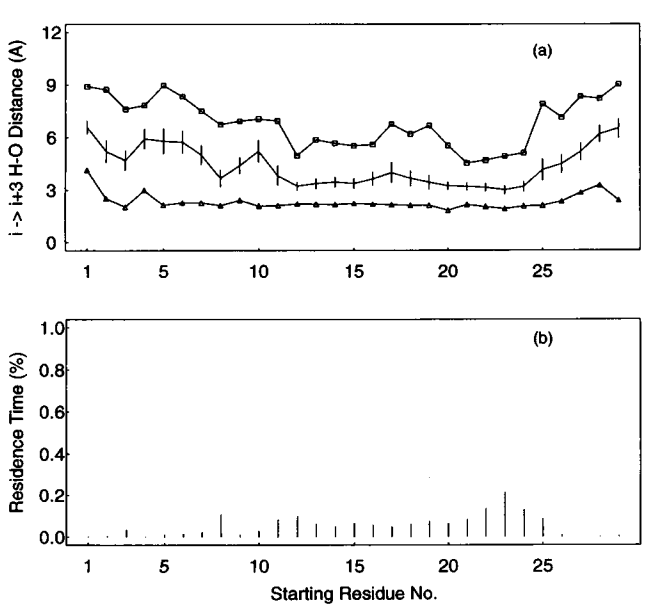

FIGURE 4 Same as in Fig. 3, except for $i \rightarrow i + 3$ H-bond distance.

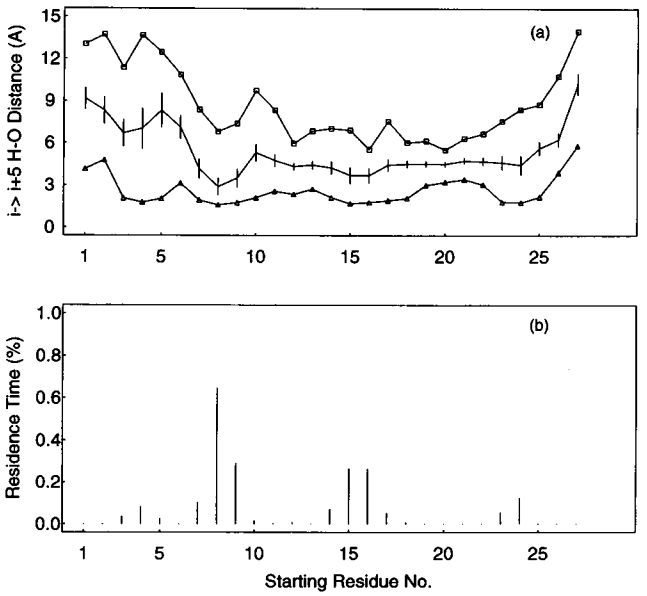

FIGURE 5 Same as in Fig. 3, except for $i \rightarrow i + 5$ H-bond distance.

Tilt and bend

The peptide was initially built as an ideal α-helix with its helical axis perpendicular to the bilayer plane. During equilibration the central part of the helix (Ala^{12}-Ala^{26}) assumed a tilt of ~10° to the bilayer normal. During the production simulation, it continued to reorient dynamically (Fig. 7), oscillating about over a range of 5° at times of tens of picoseconds and showing larger net changes in tilt over longer times of hundreds of picoseconds. Within the first 500 ps, it righted itself to 0, gradually increased to plateau at an average of ~18° for ~0.5 ns, and then increased its net tilt again, at one point achieving a value of ~30° to the normal. Note that the statistics of ϕ and ψ angles (Fig. 2) and α-helical hydrogen bond lengths (Figs. 3) for residue 17, in the very center of the helical region, underwent higher fluctuations than those of its immediate neighbors. Furthermore, visualization of the helix suggested a bending movement at this residue. To probe these phenomena further, two new helical axis were defined, Ala^{12}-Ala^{16} and Ala^{18}-Ala^{26}. Their angles with the bilayer normal (Fig. 7 *b*) show that these two segments were not always colinear and exhibited an angle of up to 50° with each other. This will be addressed

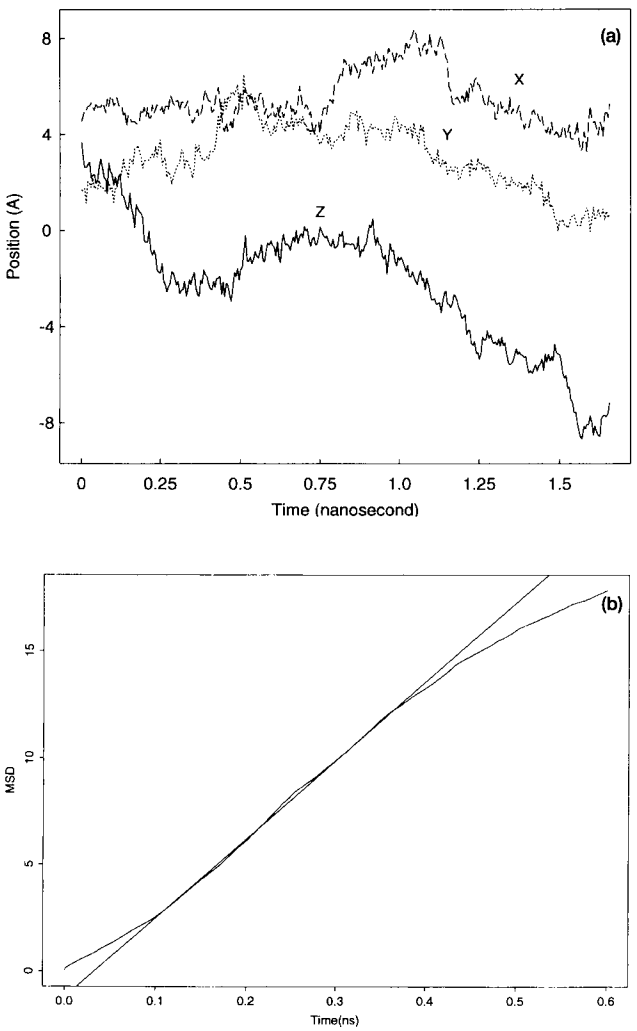

FIGURE 6 (*a*) Translation of the center mass of the $(Ala)_{32}$ in the DMPC lipid bilayer, shown by its position along the x (– – –), y (·····), and z (——) directions. (*b*) Two-dimensional lateral (within the bilayer plane) mean square displacement of the helix (*upper curve*) and the one-dimensional transverse (perpendicular to the bilayer plane) mean squared displacement (*lower curve*). The straight line marks the range of the fit used to determine the diffusion coefficient.

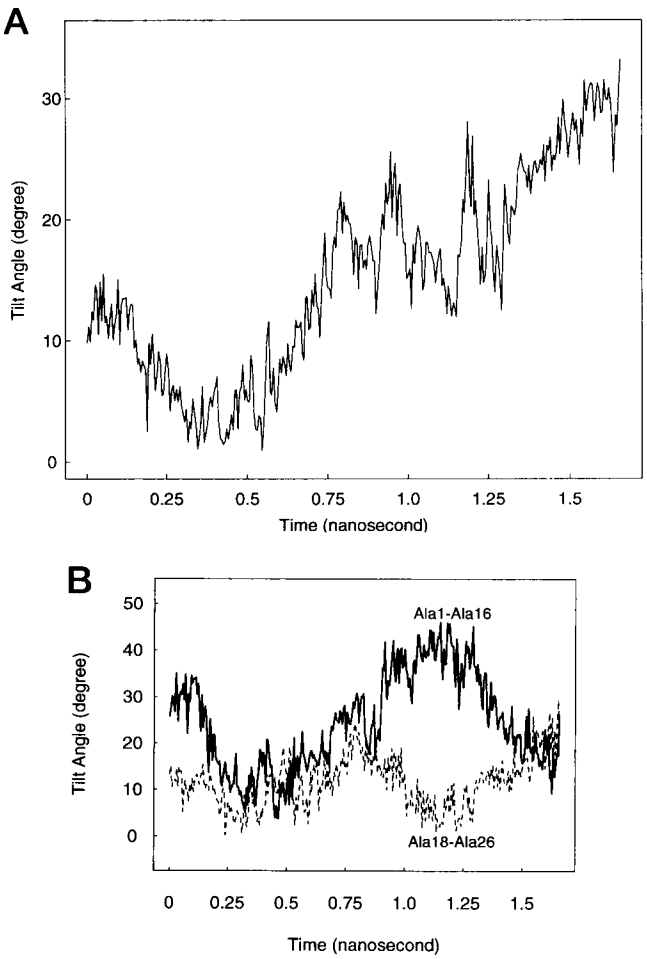

FIGURE 7 (*a*) Tilt of the helical segment, Ala^{12}-Ala^{26}, of the $(Ala)_{32}$ peptide in the DMPC lipid bilayer, measured by the angle formed between the helical axis and the bilayer normal. (*b*) Tilt of each half of the helical segment, Ala^{12}-Ala^{16} and Ala^{18}-Ala^{26}, measured by the angles of their helical axes from the bilayer normal.

further in the Discussion. It seems likely that the higher frequency local tilting was due to local atomic motions that made slight adjustments to the orientation of the best-fit line.

Rotational time correlation function

Net rotation of the helix was slow. It was further complicated by the fact that the helix was not a rigid body, as has already been shown. As before, at each time step the helical axis was determined by the line best fit to the backbone residues Ala^{12} to Ala^{26}. For each residue, the rotation was investigated by the time-dependent behavior of the vector from the C_α atom normal to the helix axis. Within the entire peptide, the rotational behavior of the individual residues was inhomogeneous, and the maximum rotational angle ranged from 25° to over 154° (Fig. 8 *a*). Even within the helical segment (Ala^{12}-Ala^{26}), the maximum rotational angles of the residues differed greatly. In particular, the N-terminal half of the helix, Ala^{12}-Ala^{18}, rotated substantially more than did residues Ala^{19}-Ala^{26}. This difference is demonstrated by the average of the rotational time correlation functions (RTCF) $((1/n)\ \Sigma_i\ \langle \cos\ \theta_0 t\ \cos\ \theta_i t \rangle$, where i is the residue number and n is the total number of residues) for the two parts of the helix (Fig. 8 *b*). The average correlation of the N-terminal part of the helix eventually decayed to zero after 1.66 ns; however, the C-terminal half showed little decorrelation. Besides illustrating the difference between the two portions of the helix, this demonstrates that accurate calculation of the rotational correlation times is probably beyond nanosecond simulations. Based on rotational relaxation time estimates of 10^{-3} to 10^{-5} s (Gennis, 1989, p. 180), this is not unexpected.

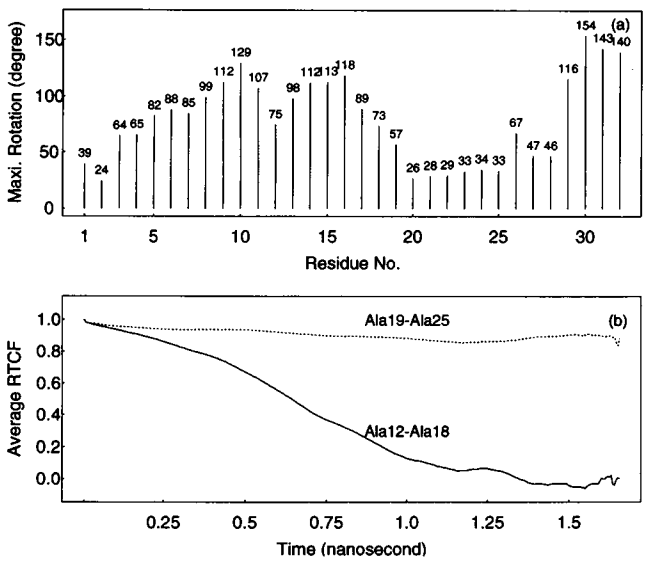

FIGURE 8 Rotational time correlation function (RTCF) for the $(Ala)_{32}$ peptide. (*a*) Maximum rotation angles for the residues over 1.66 ns. (*b*) Average values for the segments Ala^{12}-Ala^{18} and Ala^{19}-Ala^{25}.

Properties in vacuum

Clearly, the peptide experienced a wide range of motions within the membrane. To establish which of these were intrinsic to the peptide itself (because of its structure, the force field used, and the simulation conditions) and which were due to the membrane environment, a parallel 1-ns simulation was conducted of the peptide in vacuum. Statistics of the ϕ, ψ angles (Fig. 9) show that the peptide retained a stable and mostly uniform α-helix (α-helix residence times larger than 90% and 80%, respectively). Although some expected "fraying" of the helix at its ends was noticeable, this was not nearly as extreme as that seen for the N and C termini in the membrane simulation, which were exposed to the lipid headgroups and water. Hydrogen bond distances also support a helical structure (Fig. 10) that fluctuated for individual residues between the α- (Fig. 10 *b*; ~40–50% residence) and π- (Fig. 10 *c*; ~30% residence) helical forms. The 3_{10} form was seen only ~5% of the time. As with the peptide in the membrane, the transitions between helical types was reflected by the fluctuations in the helical cross-sectional radius, which fluctuated consistently

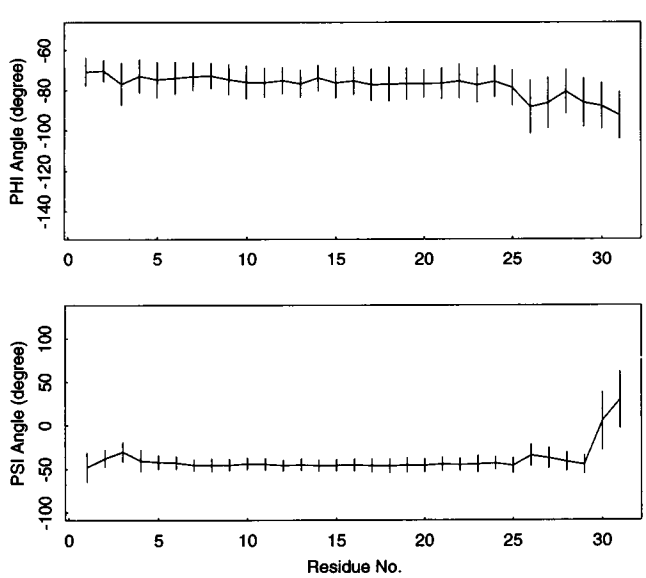

FIGURE 9 Average torsional angles (ϕ, ψ) and standard deviations (*bars*) of the $(Ala)_{32}$ peptide simulated in vacuum.

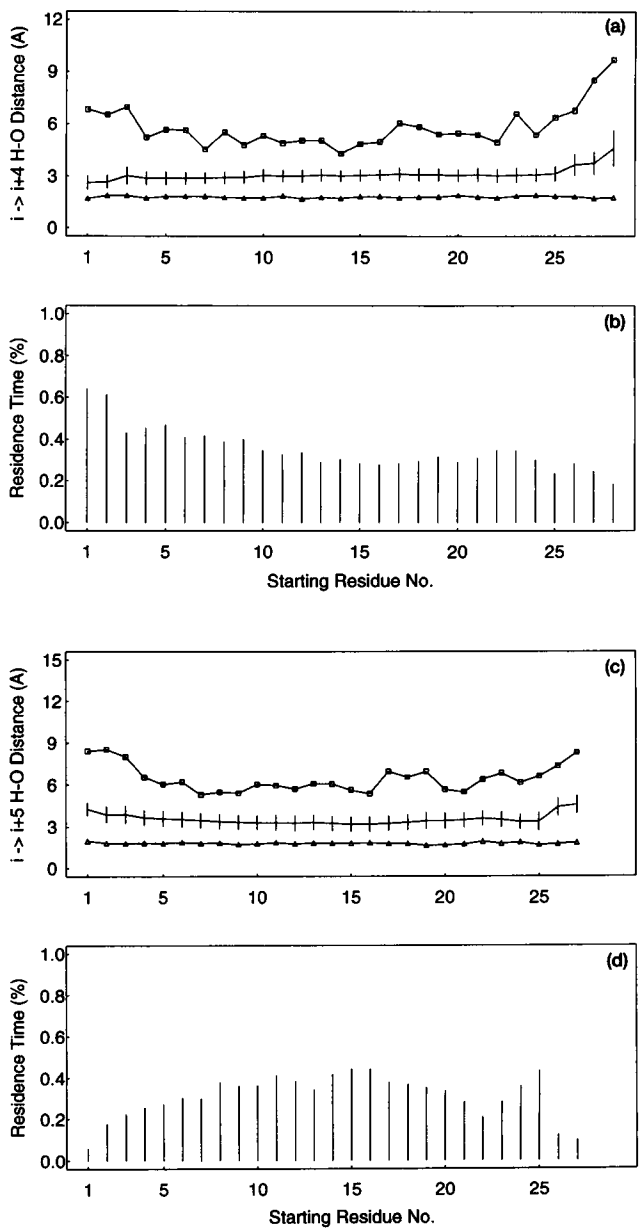

FIGURE 10 Statistics of $i \rightarrow i + 4$ H-bond distances (*a* and *b*) and $i \rightarrow i + 5$ H-bond distance (*c* and *d*) of the $(Ala)_{32}$ peptide simulated in vacuum. The solid line with bars stands for the average value and the standard deviation, and the line with squares and the line with triangles show the maximum and minimum distances observed over the 1.66-ns simulation time.

throughout the simulation in a stepwise fashion between ~2.35 Å (α) and 2.85 Å (π), the same range as seen in the membrane. Similarly, the rmsd from the ideal form ranged from 1 Å to 2.5 Å, similar to that seen within the membrane.

At the N and C termini, the fluctuation of the ϕ and ψ angles during the membrane simulation was greater than the corresponding values for the vacuum simulation, as expected because of the increased denaturation due to the interaction with water. The ϕ and ψ torsions in the most central transmembrane region in the membrane simulation tended to be slightly smaller (on average <10°) than the corresponding region in the vacuum simulation. In general, the fluctuations indicated by the standard deviation of these mean values were also slightly less when the peptide was in the membrane than when it was in vacuum. The increased stability of the helix within the membrane was made even more evident by the hydrogen bonding statistics. Within the hydrocarbon core, the average hydrogen bond distances were as much as 0.75 Å less than the corresponding values in the vacuum simulation. The standard deviations of these values in the membrane simulation were several tenths of an angstrom smaller than in vacuum, demonstrating smaller fluctuations.

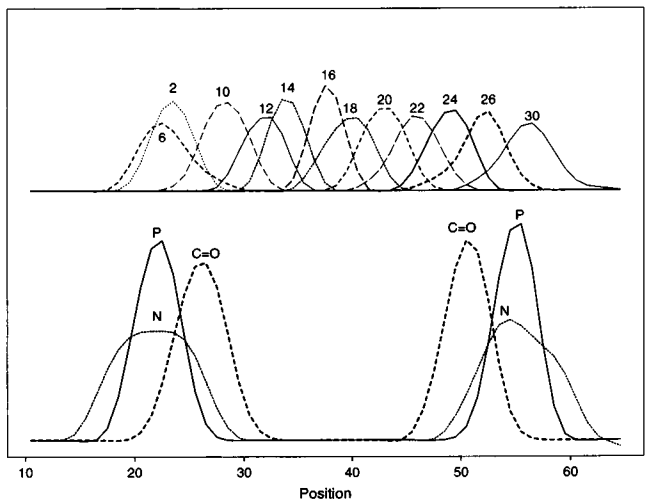

FIGURE 11 Transverse atom distributions of lipid P atoms, lipid N atoms, lipid carbonyl O atoms, as well as those of C_α atoms of $(Ala)_{32}$ residues 2, 6, 10, 12, 14, 18, 22, 24, 26, and 30, respectively.

Peptide environment

The lipid bilayer is an anisotropic environment of strong contrasts that has profound effects on even a helix as simple as polyalanine, as we have seen. Comparison of the helices' properties between vacuum and the membrane shows that the environment influences the peptide's structural and dynamical properties. This section discusses the details of the peptide's interactions with the membrane, including the lipid molecules and water.

Transverse atom distributions

Fig. 11 shows distributions of selected atoms along the bilayer normal. It clearly shows the distributions characteristic of neutron scattering studies of similar systems (Wiener et al., 1991; Wiener and White, 1991, 1992; White and Wimley, 1994). We defined the "headgroup" or polar region of the bilayer as extending from the carbonyl groups to the furthest reach of the choline groups. Based on this definition, the headgroup region is at least 15 Å wide (not accounting for layers of water ordered by the lipid molecules; Alper et al., 1993b). For an ideal α-helix of 5.4 Å rise per turn, this means that three turns of the helix (10–12 residues) could be exposed to the polar region. In actuality, because of the large concentration of water at the outermost extremes of this region, the polyalanine helix largely denatures. The helical structure is maintained through just about one-half of this region. The helix, extremely stable from residues 12 and 24, starts to become less stable upon entering the regions occupied by the carbonyl groups of the fatty ester linkages. Of course, profiles such as this include undulation in the bilayer, and so a profile such as this might suggest a contact region that is overly broad. A more detailed examination of the intimate neighborhood of the peptide will be discussed.

Specific atomic interactions

The interatomic structure around a particular atom type can be partially described by pair distribution functions that show the probability of the presence of one atom type at a particular distance from a second atom type. Fig. 12 shows a series of such functions between the peptide (the amide hydrogen and carbonyl oxygen) and the surrounding lipids and water. Fig. 12 *a* shows the pair distribution function between the peptide carbonyl oxygen and the lipid choline nitrogen. This shows a prominent peak at 4.0 Å at a probability substantially greater than random. Yet the tetraalkylammonium moiety of the choline group had no potential for hydrogen bonding. The only interaction between them was due to their opposite atomic partial charges. Choline's full positive charge was spread among the 11 hydrogens of the alkyl groups, making the charge diffuse. These close peptide carbonyl oxygen/choline nitrogen interactions occurred between the peptide and 12 of the lipid molecules during the course of the simulation. Usually this occurred for three lipid molecules in each monolayer at any one time. These interactions lasted for as long as a nanosecond or as short as 5 ps.

Fig. 12 *b* displays a low but discernible peak at 2.2 Å between the peptide carbonyl oxygen and water oxygen, indicating occasional hydrogen bonding. A second peak is also discernible at 5.5 Å, showing a second shell of water molecules. The low size of the peak is indicative of the fact that only a few of the carbonyl oxygens hydrogen bonded with water at any one time, because most are sequestered

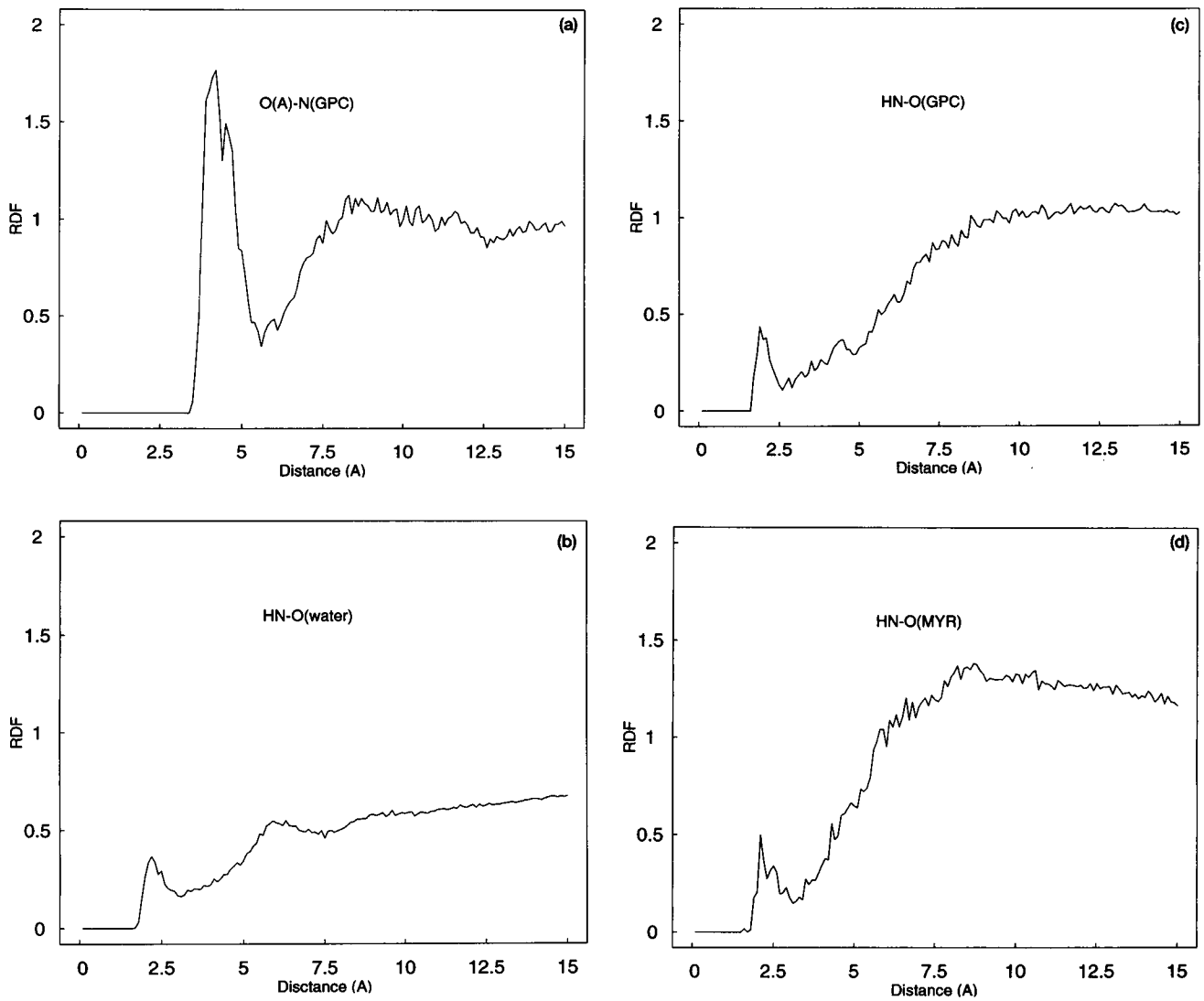

FIGURE 12 Radial distribution function (RDF) of (*a*) peptide carbonyl oxygen-lipid nitrogen; (*b*) amide hydrogen-water oxygen; (*c*) amide hydrogen phosphate oxygen; and (*d*) amide hydrogen myristoyl oxygen.

within the anhydrous membrane interior. Similar H-bonding interactions are seen between water and the peptide's amide hydrogen (plot not shown).

That the peptide interacts with water is not surprising, considering that the termini are denatured. Perhaps more interesting is the fact that through its amide hydrogen the peptide forms occasional hydrogen bonds with the lipid molecules, both with the phosphate oxygen atoms (Fig. 12 *c*) as well as with fatty acyl ester oxygen atoms (Fig. 12 *d*).

To explore these specific lipid/peptide hydrogen-bonding interactions further, Fig. 13 shows peptide amide/lipid oxygen interactions of 2.5 Å or less. Clearly, the center part of the helix formed no hydrogen bonds with the lipid molecules. Of course, this would not be expected, because the potential H-bond acceptor atoms of the lipid molecules do not penetrate deeply enough into the hydrocarbon region of the bilayer for this to happen. The deepest hydrogen-bonding interactions occurred for residue 12, which is the beginning of the most stable region of the α-helix. Its interaction was with the deepest hydrogen bond acceptor, the ester carbonyl oxygen atom. Curiously, substantially more H-bonds were formed by the N-terminal residues of the peptide than by the C-terminal residues.

Note that close to the C terminus (residue Ala^{32}) of the peptide, one lipid formed an H bond for a long period (~0.7 ns). Moreover, this lipid's choline was also a long-term neighbor of the peptide's carbonyl oxygen atoms. It seems that this lipid maintained a long-term residency with the peptide through both H bonding and polar-polar interactions. As shown in Fig. 13, other lipid molecules had more transient interactions, usually lasting no more than several hundred picoseconds. These hydrogen bonds often switched between different adjacent residues of the peptide and sometimes hydrogen bonded to several residues at one time.

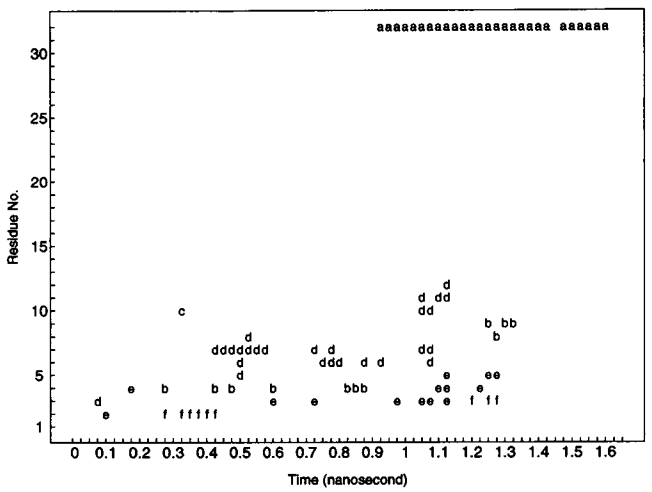

FIGURE 13 Lipid/peptide hydrogen bonds (peptide N-H to lipid O distances less than 2.5 Å). The letters shown in the plot represent the identity of the lipid involved in H bonding.

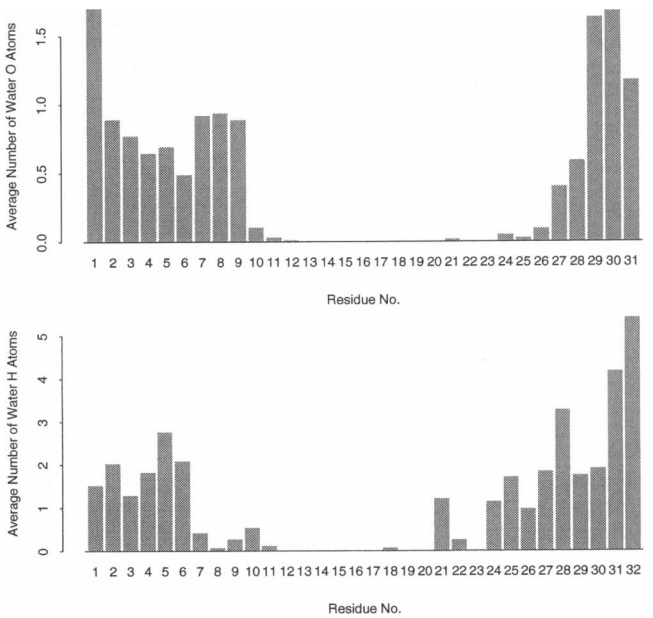

FIGURE 14 (*a*) Average number of water O atoms within 3.5 Å from amide H atom of the $(Ala)_{32}$ peptide. (*b*) Average number of water H atoms within 3.5 Å of the carbonyl O atom of the $(Ala)_{32}$ peptide.

The lipids had four possible H-bond acceptors: -P═O, -P-O-, -C═O, and -C-O-. Of the four types of potential lipid hydrogen-bond acceptor atoms, interactions with the ester ether linkage never occurred and interactions with the phosphoether oxygen atom occurred only rarely. The carbonyl oxygen atom hydrogen bonded most frequently and with a greater range of residues. Many hydrogen bonds formed with the phosphoryl oxygen; however, these were for a much smaller number of residues, which were at the termini. For the lipid molecules then, the interactions most pertinent to the helix structure and stability were with the ester carbonyl oxygens.

Of equal or perhaps even greater importance as both a hydrogen bond donor and acceptor is water. As noted above, water penetrates into the bilayer to the depth of the carbonyl groups of the lipid molecules. Fig. 14 shows the average number of water molecules neighboring the hydrogen-bonding functional groups of the peptide. On average, at least one water molecule was present from the N terminus to residue 10, and lesser amounts of water occurred as deep as residue 13. Similarly, an average of at least one water molecule occurred from residue 24 through to the C terminus. Residue 21 was also frequently neighbored by a water molecule, although because of the periodicity of the helix, this might be the same molecule as that which neighbored residue 24.

Lipid packing

Certain questions naturally arise in studies of transmembrane proteins. For instance, what are its surroundings? How many lipid molecules surround the protein? Do they pack tightly or loosely? Do these constitute a well-defined annulus? What are the residence times of these lipids?

To determine this, the number of lipid molecules present in concentric cylinders of increasing size around the peptide helix was tabulated. In a shell as small as 3 Å radius there were on average 10 lipid molecules represented. Similarly, for 5.0 Å there were 18, for 7.0 Å 22, for 9.0 Å 25, for 11.0 Å 28, for 13.0 Å 31, and for 15.0 Å 33. All of the 32 lipid molecules were present in a cylinder of ~13 Å, less than one-half the box size of 34.5 Å.

Clearly, many different lipid molecules contributed to the peptide's immediate surroundings. The peptide was not surrounded by only a few, well-packed lipid molecules. This is perhaps not surprising, considering that within the L_α phase bilayer the conformations of lipid molecules have been shown to be wide-ranging and often extended (Stouch, 1993; Pastor et al., 1991). In fact, even though a particular lipid molecule's hydrocarbon chain was immediately adjacent to the helix, its headgroup could be a substantial distance away. Considering the diameter of the helix and the size of a phosphate group, a phosphate immediately adjacent to the helix would be ~8–10 Å away from the center of the helix. In fact, on average, about five lipid molecules that had their hydrocarbon chains adjacent to the helix also had their phosphate groups within this range. However, the headgroup (as measured by the position of the phosphorus atom) was found as much as 16–18 Å away. Because the average distance between lipid headgroups in this bilayer is 8 Å, these would be considered to be in the second "shell." In fact, on average the headgroups of a number of lipid molecules existed between these extremes, further demonstrating a diffuse environment around the peptide as opposed to a well-ordered series of lipid shells. The maximum distance occurred for a lipid whose hydrocarbon chain was largely in the all-*trans* conformation and, because of a *gauche* torsion high in the chain, was almost parallel to the

TABLE 1 Distance from helix of phosphorus atoms of neighboring lipid molecules versus average number of lipid molecules

Distance range (Å)	Number of lipids
0–2	0.1
2–4	0.3
4–6	0.7
6–8	2.3
8–10	2.2
10–12	2.7
12–14	2.2
14–16	2.1
16–18	0.9
18–20	0.4
20–22	0.2
22–24	0.1

Note that these distances were to the helix axis. The smallest distance occurred for a P atom in the water where the peptide denatured and was not coincident with the axis. Substantial helix tilt allowed the computed P-helix axis distance to be small.

bilayer plane. To quantify this, at each configuration all of the lipid molecules that had at least one atom present within 5 Å of residues 12–24 (the central helix) were identified. The distance between the α-helical axis and the phosphorus atom of each of those lipids was calculated, and a histogram was prepared of the number of lipid molecules versus the distance. This was averaged over all configurations (Table 1). For example, on average the phosphorus atoms of 2.3 lipid molecules were between 6 and 8 Å of the helix center, and those of 2.1 lipid molecules were between 14 and 16 Å.

Another view of the lipid/protein packing can be gained by examination of the contribution of individual lipid molecules to the cylindrical shells surrounding the protein, described above. The time-averaged results for the 5 Å are shown in Table 2. For example, on average four lipid molecules contributed from one to five nonhydrogen atoms to the 5-Å shell; similarly, 2.4 lipid molecules contributed 6–10 atoms, 3.9 contributed 11–15 atoms, etc. The DMPC molecules contain 46 nonhydrogen atoms. The number of contributing lipid molecules drops off substantially the greater the number of atoms contributed. It is clear that this shell is composed of a large number of lipid molecules, each contributing a small number of atoms. Of the 46 heavy atoms in a DMPC molecule, only rarely does any one molecule have more than 25 atoms within this shell, demonstrating that only rarely does any one entire lipid molecule pack tightly with the helix.

TABLE 2 Average number of lipids with a given number of lipid heavy atoms within 5.0 Å of the peptide

No. of heavy atoms	Average no. of lipids
1–5	4.0
6–10	2.4
11–15	3.9
16–20	3.4
21–25	2.4
26–30	1.6
31–35	0.4
36–40	0.0

TABLE 3 Bulk properties of the membrane

	Peptide-lipid bilayer	Neat lipid bilayer
Thickness (P-P)	33 ± 2 SD Å	34 ± 2 SD Å
P-N tilt	89° ± 20°	87° ± 30°
Hydrocarbon chain torsion (no. *gauche*/chain)	2.8 ± 0.2	3.1 ± 0.2

Bulk properties of the lipid bilayer

In comparison with neat lipid bilayers (i.e., without a transmembrane helix), the gross morphological properties of the bilayer varied little, if at all (Table 3). The average thickness of the bilayer was essentially the same, whether or not the peptide was present. This does not preclude a local swelling or thinning of the bilayer with compensating effects elsewhere: however, we did not think that the statistics of the simulation warranted such a detailed examination. The lipid headgroups behave similarly—in both systems they lie approximately parallel to the bilayer plane. Commensurate with the identical thicknesses was the fact that the hydrocarbon chains displayed the same ratios of *trans* versus *gauche* rotamers. A very sensitive measure of the order of the lipid hydrocarbon chains, the order parameter of the methylene groups (experimentally derived from NMR quadrapolar splittings), decreased (decreased order in the presence of the peptide; Fig. 15), consistent with changes seen in the presence of other solutes or peptides, both in simulation (Stouch and Bassolino, 1996; Bassolino et al., 1993; Bassolino-Klimas et al., 1995; Scott, 1986) and experimentally (Jacobs and White, 1984).

Lipids

The structure and dynamics of the lipid molecules, including translation, tilt, and chain conformation, are presented below.

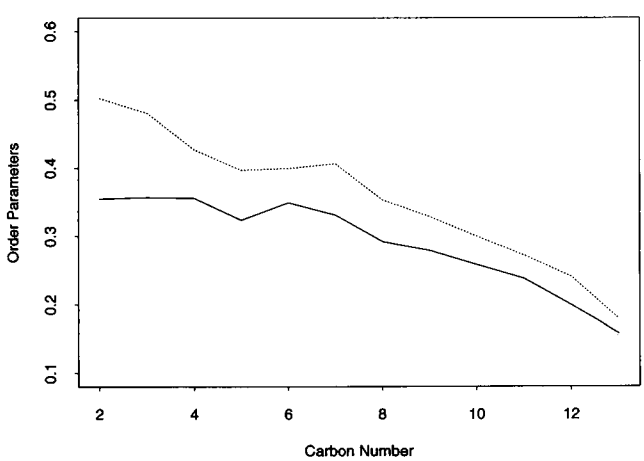

FIGURE 15 Average order parameter for two lipid hydrocarbon chains. ·····, "Neat" bilayer; ——, bilayer with $(Ala)_{32}$

Translational motion of each lipid was determined by the position of its phosphorus atom. The total movement in three dimensions for the lipid molecules over the 1.66-ns simulation ranged from 4.8 Å to 17.1 Å. However, in the direction normal to the bilayer plane, the lipid molecules translated only 4.6 Å to 9.7 Å. No doubt the limits to movement were determined by avoidance of exposure of the hydrocarbon chains to water on one side, and avoidance of dehydration of the headgroups on the other. Similar to the peptide's movements, translation of the individual lipids within the bilayer plane was much larger than that along the bilayer normal, ranging from 9.6 Å to 24.4 Å. Overall, within the plane of the bilayer, some of the lipids appeared to exhibit collective translational motion.

To understand the relative orientation and conformation of the lipid molecules, the tilts of the hydrocarbon chains and headgroup (P-N vector) from the bilayer normal were determined. The tilts of the two hydrocarbon chains were determined from the line best fit to the carbon atoms of the hydrocarbon chains. Furthermore, the angle between the two hydrocarbon chains of each lipid molecule was calculated. Table 4 summarizes these results statistically (averaged over all lipids and all times). As mentioned, the average tilt of the headgroups was 89°, nearly parallel to the bilayer, agreeing with the experimental observation (Buldt and Wohlgemuth, 1981; Seelig et al., 1977). However, for individual lipids, this varied within 69°, no doubt contributing to the broadness of the headgroup interface. The two hydrocarbon chains were, on average, 33° and 37° from the normal, in agreement with studies of the neat bilayer (Stouch, 1993). The hydrocarbon chains were almost perpendicular to the headgroup P-N vector (mean angles of 93° and 95°) and at a 36° to each other. However, like the headgroups, the ranges in values were large.

The variation of these values within individual lipid molecules is important to understanding the dynamics and responsiveness of the system. The maxima and minima of these quantities are also presented in Table 3. One sees that lipid tilt angles could differ significantly with time. For example, for the headgroups the minimum variation of the tilt was at least 44°, and the maximum change was as large as 144°.

TABLE 4 Average tilt and bend of the lipid three chains

	Mean	Max. diff.	Max. vari.	Min. vari.
P-N vector tilt	89°	69°	144°	44°
MRY1 tilt	33°	52°	115°	33°
MRY2 tilt	37°	63°	90°	34°
(P-N,MRY1) bend	93°	100°	174°	69°
(P-N,MRY2) bend	95°	87°	172°	70°
(MRY1,MRY2) bend	36°	58°	157°	37°

Here the P-N vector was used to represent the headgroup, and the best fitted axes were used for the two hydrocarbon chains. The tilt and bend of the three chains of the lipids were then calculated by the orientations of these three axes. The first three columns of data are the summary over all the lipids. And the last two columns are the results observed during the simulation among the individual lipids.

The end-to-end distances of the fatty acyl chains were used as a simple way to describe chain conformation. Fig. 16 displays the statistics of these distances for the 64 hydrocarbon chains. The average C_1-C_{14} distance was ~14 Å, but varied from ~10 Å to 15 Å. The length of individual hydrocarbon chains varied by as much as 12 Å. Several chains achieved distances of only 4 Å, which corresponds to hairpin structures that bring the terminal methyl group of the chain to the headgroup region, a phenomenon also seen previously (Stouch, 1993). This shows that not only did the hydrocarbon chains as a whole experience an abundant range of conformations, but also that individual chains did so during the course of the simulation.

The mean length of ~14 Å, coupled with the mean tilt of ~35° over both monolayers, explains the hydrophobic core thickness of the bilayer, which was ~24 Å.

DISCUSSION

The fluidity of the bilayer, caused by the conformational flexibility of the lipid molecules and the water-mediated lipid-lipid interactions, results in substantial disorder and a broad and fluctuating water/membrane interface. White has described the headgroup region as being one of "tumultuous chemical heterogeneity" (Wiener and White, 1992; White and Wimley, 1994). We define this region as that of contact between water and the lipid molecules. By this definition, it extends from the partly hydrated carbonyl groups of the fatty acyl linkages to the choline moieties, which are the portions of the lipid molecules that penetrate farthest into the water. When viewed from the side of the bilayer, this region can be over 15 Å. The breadth is due not only to the conformational flexibility of the lipids, but also to the fact

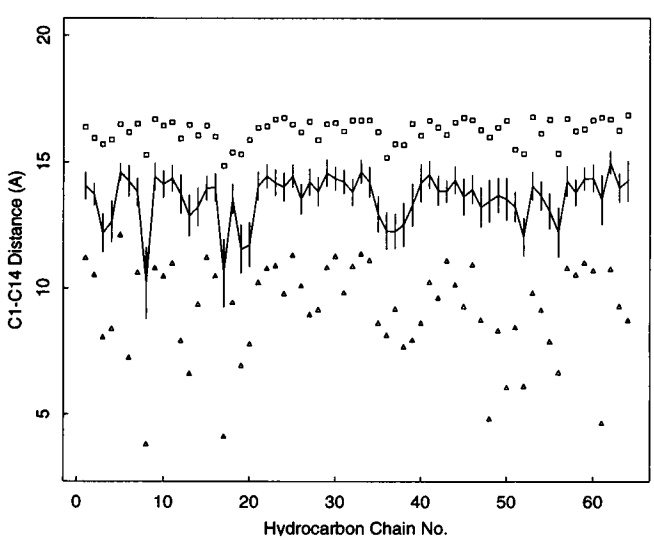

FIGURE 16 C1-C14 distance of intra-lipid hydrocarbon chains (even chain number for Myr1 and odd for Myr2). The solid line with bars stands for the average value and the standard deviation, and the open squares and the triangles show, respectively, the maximum and minimum distances observed over the 1.66-ns simulation time.

that their transverse position can vary by several angstroms. Because of this, the local environment around a TM protein might not experience the full breadth of the interface. However, we still saw at least two turns of the helical region of the peptide interacting with the lipids and water in the headgroup region. When these are combined with the denatured most terminal ends of the peptide, 11 N-terminal residues and 7 C-terminal residues are in the headgroup or water regions.

It is common to consider a TM helix as being ~20 residues in length. In our simulation, ~24 residues of the 32-mer were helical a substantial fraction of the time. The 12 central-most residues, those that interacted only with the hydrocarbon chains, formed a very stable helix. As soon as the "headgroup" region was entered, the helix became less stable and fluctuated more, because of transient hydrogen bonds with the acyl carbonyl groups and water. Increased fluctuations at the ends of helices ("frayed ends") are commonly seen both by simulation and experiment (Miick et al., 1993; Vogel et al., 1988; Daggett and Levitt, 1992; Zhang et al., 1995a; Daggett et al., 1991). Furthermore, fluorescence anisotropy measurements and amide hydrogen exchange experiments have identified even greater fraying at the ends of TM proteins (Vogel et al., 1988; Zhang et al., 1995a), such as we show here. Although some of the hydrogen bonds between the peptide and the lipid carbonyl groups persisted for hundreds of picoseconds, they were not so strong or so frequent that they denatured the helix. Once the lipid-peptide hydrogen bonds were broken, the helix was readily remade. As mentioned, this largely helical state continued for about two more turns (approximately six residues), after which the then largely aqueous environment prevented the helix from reforming and a random coil state predominated.

In comparison to the vacuum calculation, the membrane environment had a substantial influence on the helix structure and dynamics. As noted, the water/headgroup interface substantially denatured the most terminal ends of the peptide, whereas only slight fraying was noted in vacuum. In vacuum, the torsion angles showed a homogeneous profile, in contrast to that for the membrane, which although homogeneous for the central 12 residues, gradually becomes less stable as the termini are approached. In the hydrocarbon core of the bilayer, the center of the helix is more stable than in vacuum, as evidenced by the shorter hydrogen bonds and the smaller torsional fluctuations. In vacuum, the employed force field provides for a π-helix for a length of time almost equivalent to that it spends in the α form, and almost none of the 3_{10} form is seen. In contrast, in the bilayer simulation, the peptide showed only a small percentage of the π-helix, and that in isolated positions. The α-helix was by far most prevalent. A small amount of 3_{10}-helix was seen, but substantially more than in vacuum. It is unlikely that the cause of these shifts is due to "hydrophobic mismatch" or specific peptide/membrane interactions, because the alanine residues are essentially featureless and the peptide is homogeneous. Rather, it appears that the membrane environment creates a preference for the longer, tighter, helical forms, such as has been suggested previously for peptides in hydrophobic environments (Smythe et al., 1993).

Although we have not included the results here, during a simulation of the peptide in water, the peptide lost most of its helical character after several hundred picoseconds, a result also seen in other laboratories (Daggett and Levitt, 1992).

Interconversion between different helical forms has commonly been seen in both experimental and theoretical studies of helices (Miick et al., 1993; Smythe et al., 1993; Pleiss and Jahnig, 1991; Van Buuren and Berendsen, 1993; Zhang et al., 1995a,b). This was seen here, both in the membrane and in vacuo. Although the α form was predominant, the 3_{10} and π forms were also transiently observed by monitoring $i \rightarrow i + 3$ and $i \rightarrow i + 5$ hydrogen bonds in addition to the α-helical $i \rightarrow i + 4$ hydrogen bond. This was also reflected in the radius of the helical cross section as well as the helix length. The fluctuations between helical forms were generally local in nature and usually did not extend more than a few residues. However, apparently initiated by a large movement of the disordered N-terminal region, one large rotation did occur that propagated along the helix, dampening with distance. This directly resulted in a 90° rotation of the N terminus, an average (for the entire peptide) 0.2-Å increase in cross section, an average 1.3-Å shortening of the helix, and formation of π ($i \rightarrow i + 5$) hydrogen bonds. Similar fluctuations in length and cross section have been observed in previous simulations of polyalanine (Vogel et al., 1988; Daggett and Levitt, 1992; Zhang et al., 1995b) and decaglycine (Perahia et al., 1990).

It is interesting to speculate just how Nature might use these facts. For example, it is conceivable that a helix-destabilizing sequence, coupled with the helix-destabilizing nature of the headgroup region, could result in a helix shorter than the commonly accepted 20 residues for a TM helix. Similarly, a helix-stabilizing sequence could be employed to allow the helix to extend further into the headgroup region. It has been proposed that the rules of secondary structure formation are different between globular and TM proteins (Li and Deber, 1994). It is possible that the rules might be intermediate or even completely different in the unique headgroup environment.

The helix was found to tilt substantially, on average 32° but ranging from 0° to 45°. In fact, there is little reason not to tilt, because there were no residues that would have strong, irreplaceable contacts with the headgroup or aqueous regions. In fact, tilting would allow a maximization of the hydrophobic interactions by allowing more of the hydrophobic alanine residues to interact with the bilayer hydrocarbon core. That more tilting did not occur might be due to favorable hydrogen bonding interactions formed by the denatured terminal residues. Greater tilt might require some residues to relinquish favorable electrostatic interactions or hydrogen bonds for the nonpolar environment of the membrane interior. The energetically favorable alternative to this, replacement of those contacts with intramolecular hy-

drogen bonds, would be entropically disfavored. A similar argument can be applied to rationalize the limited transverse translational movement of the helix. Perhaps also, less tilt would be favored by interactions between the membrane dipole potential (previously seen to be due partly to ordered water molecules; Alper et al., 1993b; Gawrisch et al., 1992) and the helix dipole. The tilt, along with the homogeneous nature of the helix, might also be the reason that no evidence was seen of bilayer thickening, as suggested by the hydrophobic mismatch hypothesis (Zhang et al., 1995b; Sperotto and Mouritsen, 1991).

The helix assumed a variety of bends. Some appeared to be distributed along the helix, a portion of the bend shared by each residue. However, many were focused at residue 17, as reflected by its higher mobility (ϕ, ψ and H-bond fluctuations greater than the neighboring residues). Residue 17 resided in the center of the bilayer. It is well known that this is a region of low density and high disorder (Wiener et al., 1991; Wiener and White, 1992; Seelig et al., 1977; White and Wimley, 1994; Seelig and Seelig, 1974, 1977; Stouch, 1993). Interconversions between straight and bent (or kinked) helices were observed previously for polyalanine helices (Pleiss and Jahnig, 1992; Daggett et al., 1991). It is interesting to speculate whether the "hinge" motion of this residue is due in part to this lower density and whether its position would be shifted in proteins of different sequence. Many TM proteins contain prolines in postulated helical regions, which would further destabilize a helix. It has been suggested that these prolines might play a role in signal transduction. Less obvious sequence variations might also result in differences in movement.

The substantial lateral translation of the helix has been noted. Visual inspection of the trajectory showed a correlation between this translation and the bending motion at residue 17. This correlation can be combined with the "hole-jumping" hypothesis of diffusion to suggest a mechanism of translation. This hypothesis states that for a molecule to move to a new position, a neighboring molecule must first move to free the volume into which the first molecule moves. In a bilayer, the two monolayers are not correlated in their movements, however. It is unlikely that if a lipid molecule moves away from the helix in one monolayer, an identical event would occur at the same instant in the other. This would result in translation of each half of the helix separately, culminating in some strain and bending.

The calculated lateral diffusion coefficient of 9.7×10^{-7} cm^2/s is 10–15 times faster than those measured for larger proteins, such as glycophorin and rhodopsin in phospholipid vesicles (Edidin, 1981, p. 37; Jacobson, 1983). This might be expected, because this peptide is substantially smaller and lacks either hydrophilic or hydrogen-bonding amino acids or glycosylation. It is also very likely that in the short 1.66 ns of this simulation, we are sampling only short-scale, "rattling in a cage" motion. Quasielastic neutron scattering, the time scales of which are comparable to those of this simulation, finds diffusion of lipid molecules in the L_α phase 100 times faster (10^{-6} cm^2/s) than do methods covering a longer time scale, such as fluorescence recovery after photobleaching (10^{-8} cm^2/s) (Vaz and Almeida, 1991, and references therein). It could also be partly artifactual, because of the limited sampling of diffusional data during the 1.6-ns simulation.

Except for a decrease in order parameters, the bilayer properties, lipid conformations, lipid lateral diffusion rates, and headgroup orientations were essentially identical to those of a neat bilayer (Stouch, 1993). As reflected by the order parameters, the protein did not induce an ordered layer of lipids around the protein. Although an ordering of the hydrocarbon chains was seen at some methylene groups during a relatively short simulation of a TM polyglycine helix, the rougher glycophorin helix showed substantially less ordering during the same study (Edholm and Johansson, 1987). Scott reported Monte Carlo studies of stylized representation of TM helices in bilayers that, similar to our results, showed a lowering of order parameters at methylene groups 3 and 4 for hydrocarbon chains bordering the helix representations (Scott, 1986). The order parameters for the neat bilayer (before insertion of the peptide) reproduce well experimentally determined order parameters. As the available surface area is increased, one would expect the order parameters to decrease. It is possible that the decrease in order parameters seen here might also reflect an excessive surface area for the polyalanine helix rather than an effect on the hydrocarbon chains by the helix, as assumed here and by the other, referenced, studies. However, our studies comparing surface area and order parameters suggest that for the magnitude of the shift in values seen here, the excess surface area would have to be substantially more than we would expect.

Similarly, no evidence was found for a defined "annulus" of lipids around the protein. In fact, the great conformational freedom of the hydrocarbon chains is such that the immediate neighborhood of the helix was populated by atoms not from a few tightly held lipid molecules, but from many lipid molecules, some two to three lipid layers away (based on headgroup-to-helix axis distances). This possibility should be considered during interpretation of experiments employing lipids containing labels. This same conclusion was reached in early studies of TM helices (Edholm and Johansson, 1987; Scott, 1986). A lattice-based model of a bilayer that included smooth wall cylinders suggested that a very long "coherence" length was imparted to the lipids by TM helices at temperatures near the gel-to-liquid crystal phase transition (Sperotto and Mouritsen, 1991). However, the magnitude of this perturbation decreased dramatically with increasing temperature. At a temperature of 20° above the transition, as was used here, the perturbation was predicted to extend no more than a few angstroms.

As we noted in the Introduction, this study of polyalanine is meant to be a simple benchmark by which to evaluate bilayer/TM helix interactions, as well as a point of reference against which to evaluate more complex sequences. Naturally occurring type I TM helices contain a diversity of hydrophobic amino acids. Necessarily, these will be larger

and more complex than alanine. Because of the increased bulk one might expect slower rotation and translation. Moreover, bulkier side chains might result in less interaction between the helix backbone and the ester carbonyls and headgroups. Rougher, less regular helices might also result in a futher decrease in order parameters, as suggested previously (Edholm and Johansson, 1987). Furthermore, type I TM helices usually contain hydrophilic and charged amino acids just beyond their hydrophobic cores. Because of hydrogen bonding with the lipids, such amino acids might serve to "anchor" the helices, resulting in less tilt. For example, we have found that interfacial tryptophan residues substantially retard tilting (unpublished results). Finally, it stands to reason that the stability of the helix will depend not only on interations with the bilayer, but on the nature of the sequence.

CONCLUSIONS

A multi-nanosecond MD simulation of a simple 32-residue polyalanine transmembrane helix through a hydrated DMPC bilayer was conducted as a benchmark with which to interpret future studies of more complex transmembrane proteins. The influence of the membrane environment was gauged by comparison to a parallel simulation in vacuum. The membranous environment was found to have a strong influence on the structure and dynamics. Toward the outer regions of the lipid headgroups, where a substantial amount of water exists, the peptide was denatured. Within the hydrocarbon core of the bilayer, the 12 central residues of the helix were more stable than in vacuum. Between these two regions, the lipid carbonyl groups and the water that accompanies them form transient hydrogen bonds to the peptide backbone, destabilizing—but not denaturing—the helix. In the membrane the peptide assumed a substantially greater fraction of α and 3_{10} helical forms than it does in vacuum, where the π-helical form was present 30% of the time. A frequent bend was noted at the very center of the helix, in the least dense region of the membrane. Bending at this position appeared to correlate with lateral translation. During the simulation, the helix spontaneously assumed a range of tilts relative to the bilayer plane, from perpendicular to 30°.

The authors thank J. J. Villafranca and J. Novotny for their support of this research, and Richard Shaginaw (Bristol-Myers Squibb High Performance Computing Center), John Stringer (Cray Research), and Stewart Samuels (Bristol-Myers Squibb Macromolecular Modeling Department), who played key roles in our work by orchestrating, updating, and maintaining our Cray C94 and Silicon Graphics computing network. Also, thanks to R. Pastor for helpful discussions regarding error analysis in diffusion calculations.

REFERENCES

Alper, H. E., D. Bassolino, and T. R. Stouch. 1993a. The limiting behavior of water hydrating a phospholipid monolayer: a computer simulation study. *J. Chem. Phys.* 99:5547–5559.

Alper, H. E., D. A. Bassolino, and T. R. Stouch. 1993b. Computer simulations of a phospholipid monolayer/water system: the effect of long range forces on water structure and dynamics. *J. Chem. Phys.* 98: 9798–9807.

Alper, H. E., and T. R. Stouch. 1995. Structure, interactions, and diffusion of a drug analog in biomembranes. *J. Chem. Phys.* 99:5724–5731.

Auffinger, P., S. Louise-May, and E. Westhof. 1996. Molecular dynamics simulations of the anticodon hairpin of tRNA: structuring effects of C-H···O hydrogen bonds and of long-range hydration forces. *J. Am. Chem. Soc.* 118:1181–1189.

Bareman, J. P., R. I. Reid, A. N. Hrymak, and T. A. Kavassalis. 1993. Estimation of solvent diffusion coefficients using molecular dynamics simulations. *Mol. Simul.* 11:242–250.

Bassolino, D., H. E. Alper, and T. R. Stouch. 1993. Solute diffusion in lipid bilayer membranes: an atomic level study by molecular dynamics simulation. *Biochemistry.* 32:12624–12637.

Bassolino-Klimas, D., H. E. Alper, and T. R. Stouch. 1995. Mechanism of solute diffusion through lipid bilayer membranes by molecular dynamics simulation. *J. Am. Chem. Soc.* 117:4118–4129.

Berendsen, H. J. C., J. P. M. Postma, W. F. van Gunsteren, A. DiNola, and J. R. Haak. 1984. Molecular dynamics with coupling to an external bath. *J. Chem. Phys.* 81:3684–3690.

Brooks, C. L., M. Karplus, and B. M. Pettitt. 1988. Proteins: a theoretical perspective of dynamics, structure, and thermodynamics. John Wiley and Sons, New York.

Buldt, G., and R. Wohlgemuth. 1981. The headgroup conformation of phospholipids in membranes. *J. Membr. Biol.* 58:81–100.

Challou, N., E. Goormaghtigh, V. Cabiaux, K. Conrath, and J. M. Ruysschaert. 1994. Sequence and structure of the membrane-associated peptide of glycophorin A+. *Biochemistry.* 33:6902–6910.

Cheatham, T. E., J. L. Miller, T. Fox, T. A. Darden, and P. Kollman. 1995. Molecular dynamics simulations of solvated biomolecular systems: the particle mesh Ewald method leads to stable trajectories of DNA, RNA, and proteins. *J. Am. Chem. Soc.* 117:4193–4194.

Chiu, S.-W., M. Clark, V. Balaji, S. Subramaniam, H. L. Scott, and E. Jakobsson. 1995. Incorporation of surface tension into molecular dynamics simulation of an interface: a fluid phase lipid bilayer membrane. *Biophys. J.* 69:1230–1245.

Cross, T. A., and S. J. Opella. 1994. Solid-state NMR structural studies of peptides and proteins in membranes. *Curr. Opin. Struct. Biol.* 4:574–581.

Daggett, V., P. Kollman, and I. Kuntz. 1991. A molecular dynamics simulation of polyalanine: an analysis of equilibrium motions and helix-coil transitions. *Biopolymers.* 31:1115–1134.

Daggett, V., and M. Levitt. 1992. Molecular dynamics simulations of helix denaturation. *J. Mol. Biol.* 225:1121–1138.

Damodaran, K. V., K. M. Merz, and B. P. Gaber. 1992. Structure and dynamics of the dilaurylphosphatidylethanolamine lipid bilayer. *Biochemistry.* 31:7656–7664.

Dauber-Osguthorpe, P., V. A. Roberts, D. J. Osguthorpe, J. Wolff, M. Genest, and A. T. Hagler. 1988. Structure and energetics of ligand binding to proteins: *Escherichia coli* dihydrofolate reductase-trimethoprim, a drug-receptor system. *Proteins Struct. Funct. Genet.* 4:31–47.

de Jongh, H. H. J., E. Goormaghtigh, and J. A. Killian. 1994. Analysis of circular dichroism spectra of oriented protein-lipid complexes: toward a general application. *Biochemistry.* 33:14521–14528.

Edholm, O., and J. Johansson. 1987. Lipid bilayer polypeptide interactions studied by molecular dynamics simulation. *Eur. Biophys. J.* 14:203–209.

Edidin, M. 1981. Molecular motions and membrane organization and function. *In* Membrane Structure. J. B. Finean and J. B. Michell, editors. Elsevier, New York. 37–82.

Egberts, E., and H. J. C. Berendsen. 1988. Molecular dynamics simulation of a smectic liquid crystal with atomic detail. *J. Chem. Phys.* 89: 3718–3732.

Essex, J. W., M. M. Hann, and W. G. Richards. 1994. Molecular dynamics simulation of a hydrated phospholipid bilayer. *Philos. Trans. R. Soc. Lond. Biol.* 344:239–260.

Feller, S. E., and R. W. Pastor. 1996. On simulating lipid bilayers with an applied surface tension: periodic boundary conditions and undulations. *Biophys. J.* 71:1350–1355.

Feller, S. E., Y. Zhang, and R. W. Pastor. 1995. Computer simulation of liquid/liquid interfaces. II. Surface tension-area depdenence of a bilayer and monolayer. *J. Chem. Phys.* 103:10267–10276.

Gawrisch, K., D. Ruston, J. Zimmerberg, V. A. Parsegian, P. R. Rand, and N. Fuller. 1992. Membrane dipole potentials, hydrations forces, and the ordering of water at membrane surfaces. *Biophys. J.* 61:1213–1223.

Gennis, R. B. 1989. Biomembranes, molecular structure and function. *In* Springer Advanced Texts in Chemistry. C. R. Cantor, editor. Springer-Verlag, New York. 533.

Goormaghtigh, E., and J. M. Ruysschaert. 1990. Polarized attenuated total reflection infrared spectroscopy as a tool to investigate the conformation and orientation of membrane components. *In* Molecular Description of Biological Membranes by Computer Aided Conformational Analysis. R. Brasseur, editor. CRC Press, Boca Raton, FL. 285–329.

Guba, W., R. Haebner, G. Breipohl, S. Henke, J. Knolle, V. Santagada, and H. Kessler. 1994. A novel combined approach of NMR and molecular dynamics within a biphasic membrane mimetic: conformation and orientation of the bradykinin antagonist Hoe 140. *J. Am. Chem. Soc.* 116:7532–7540.

Hagler, A. T., S. Lifson, and P. Dauber. 1979a. Consistent force field studies of intermolecular forces in hydrogen bonded crystals. II. A benchmark for the objective comparison of alternative force fields. *J. Am. Chem. Soc.* 101:5122–5130.

Hagler, A. T., P. S. Stern, and S. Lifson, Ariel, S. 1979. Urey–Bradley force field, valence force field, and ab initio study of intramolecular forces in tri-tertbutyl-methane and isobutane. *J. Am. Chem. Soc.* 101: 813–819.

Heller, H., M. Schaefer, and K. Schulten. 1993. Molecular dynamics simulation of a bilayer of 200 lipids in the gel and in the liquid-crystal phases. *J. Phys. Chem.* 97:8343–8360.

Hu, W., N. D. Lazo, and T. A. Cross. 1995. Tryptophan dynamics and structural refinement in a lipid bilayer environment: solid state NMR of the gramicidin channel. *Biochemistry.* 34:14138–14146.

Huang, P., J. J. Perez, and G. H. Loew. 1994. Molecular dynamics simulations of phospholipid bilayers. *J. Biol. Struct. Dyn.* 11:927–956.

Jacobs, R. E., and S. H. White. 1984. Behavior of hexane dissolved in DMPC bilayers: an NMR and calorimetric study. *J. Am. Chem. Soc.* 106:915–920.

Jacobson, K. 1983. Lateral diffusion in membranes. *Cell Motil.* 3:367–373.

Killian, J. A. 1992. Gramicidin and gramicidin-lipid interactions. *Biochim. Biophys. Acta.* 1113:391–425.

Killian, J. A., A. M. P. D. Jong, J. Bijvelt, A. J. Verkleij, and B. d. Kruijff. 1990. Induction of non-bilayer lipid structures by functional signal peptides. *EMBO J.* 9:815–819.

Kitson, D. H., F. Avbelj, J. Moult, D. T. Nguyen, J. E. Mertz, D. Hadzi, and A. T. Hagler. 1993. On achieving better than 1-Angstrom accuracy in a simulation of a large protein: *Streptomyces griseus* protease A. *Proc. Natl. Acad. Sci. USA.* 90:8920–8924.

Kovacs, H., A. E. Mark, J. Johansson, and W. F. v. Gunsteren. 1995. The effect of environment on the stability of an integral membrane helix: molecular dynamics simulations of surfactant protein C in chloroform, methanol and water. *J. Mol. Biol.* 247:808–822.

Lau, K., H. Alper, T. Thacher, and T. Stouch. 1994. Effects of switching functions on the behavior of liquid water in molecular dynamics simulations. *J. Phys. Chem.* 94:8587–8791.

Li, S., and C. Deber. 1994. A measure of helical propensity for amino acids in membrane environments. *Struct. Biol.* 1:368–373.

Loncharich, R. J., and B. R. Brooks. 1989. The effects of truncating long-range forces on protein dynamics. *Proteins Struct. Funct. Genet.* 6:32–45.

Marrink, S. J., M. Berkowitz, and H. J. C. Berendsen. 1993. Molecular dynamics simulation of a membrane/water interface: the ordering of water and its relation to the hydration force. *Langmuir.* 9:3122–3131.

McCammon, J. A., and S. C. Harvey. 1987. Dynamics of Protein and Nucleic Acids. Cambridge University Press, Cambridge.

Miick, S. M., K. M. Casteel, and G. L. Millhauser. 1993. Experimental molecular dynamics of an alanine-based helical peptide determined by spin label electron spin resonance. *Biochemistry.* 32:8014–8021.

Milik, M., and J. Skolnick. 1993. Insertion of peptide chains into lipid membranes: an off-lattice Monte Carlo dynamics model. *Proteins Struct. Funct. Genet.* 15:10–25.

Muller-Plathe, F., S. C. Rogers, and W. F. van Gunsteren. 1992. Computational evidence for anomalous diffusion of small molecules in amorphous polymers. *Chem. Phys. Lett.* 199:237–243.

Nagle, J. F. 1993. Area/lipid of bilayers from NMR. *Biophys. J.* 64: 1476–1481.

Nagle, J. F., R. Zhang, S. Tristram-Nagle, W. Sun, H. I. Petrache, and R. M. Suter. 1996. X-ray structure determination of fully hydrated L-α phase dipalmitoylphosphatidylcholine bilayers. *Biophys. J.* 70: 1419–1431.

Pant, P. V. K., and R. H. Boyd. 1993. Molecular dynamics simulation of diffusion of small penetrants in polymers. *Macromolecules.* 26: 679–686.

Pastor, R. W., R. M. Venable, and M. Karplus. 1991. Model for the structure of the lipid bilayer. *Proc. Natl. Acad. Sci. USA.* 88:892–896.

Perahia, D., R. M. Levy, and M. Karplus. 1990. Motions of an α-helical polypeptide: comparison of molecular and harmonic dynamics. *Biopolymers.* 29:645–677.

Pink, D. A., K. S. Ramadurai, and J. R. Powell. 1993. Computer simulation of lipid diffusion in a two-component bilayer. The effect of adsorbing macromolecules. *Biochim. Biophys. Acta.* 1148:197–208.

Pleiss, J., and F. Jahnig. 1991. Collective vibrations of an α-helix: a molecular dynamics study. *Biophys. J.* 59:795–804.

Pleiss, J., and F. Jahnig. 1992. Conformational transition of an α-helix studied by molecular dynamics. *Eur. Biophys. J.* 21:63–70.

Raghaven, K., M. R. Reddy, and M. L. Berkowitz. 1992. A molecular dynamics study of the structure and dynamics of water between DLPE bilayers. *Langmuir.* 8:233–240.

Schreiber, H., and O. Steinhauser. 1992. Taming cut-off induced artifacts in molecular dynamics studies of solvated polypeptides: the reaction field method. *J. Mol. Biol.* 228:909–923.

Scott, H. L. 1986. Monte Carlo calculations of order parameter profiles in models of lipid-protein interaction in bilayers. *Biochemistry.* 25: 6122–6126.

Seelig, J., H. Gally, and R. Wohlgemuth. 1977. Orientation and flexibility of the choline head group in phosphatidylcholine bilayers. *Biochim. Biophys. Acta.* 467:109–119.

Seelig, J., S. Nebel, P. Ganz, and C. Bruns. 1993. Electrostatic and nonpolar peptide-membrane interactions. Lipid binding and functional properties of somatostatin analogues of charge $Z = +1$ to $Z = +3$. *Biochemistry.* 32:9714–9721.

Seelig, A., and J. Seelig. 1974. The dynamic structure of fatty acyl chains in a phospholipid bilayer measured by deuterium magnetic resonance. *Biochemistry.* 13:4839–4845.

Seelig, A., and J. Seelig. 1977. Effect of a single *cis* double bond on the structure of a phospholipid bilayer. *Biochemistry.* 16:45–50.

Shinoda, W., T. Fukada, S. Okazaki, and I. Okada. 1995. Molecular dynamics simulation of the dipalmitoylphosphatidylcholine (DPPC) lipid bilayer in the fluid phase using the Nose-Parrinello-Rahman NPT ensemble. *Chem. Phys. Lett.* 232:308–322.

Smith, P. E., and B. M. Pettitt. 1991. Peptides in ionic solutions: a comparison of the Ewald and switching function techniques. *J. Chem. Phys.* 95(11):8430–8441.

Smythe, M. L., S. E. Huston, and G. R. Marshall. 1993. Free energy profile of a 3(10) to α-helical transition of an oligopeptide in various solvents. *J. Am. Chem. Soc.* 115:11594–11595.

Sperotto, M. M., and O. G. Mouritsen. 1991. Monte Carlo simulation studies of lipid order parameter profiles near integral membrane proteins. *Biophys. J.* 59:261–270.

Stouch, T. R. 1993. Lipid membrane structure and dynamics studied by all-atom molecular dynamics simulations of hydrated phospholipid bilayers. *Mol. Simul.* 10:317–345.

Stouch, T. R., H. E. Alper, and D. Bassolino. 1994. Supercomputing studies of biomembranes. *Int. J. Supercomput. Appl.* 8:6–23.

Stouch, T. R., and D. Bassolino. 1996. Movement of small molecules in lipid bilyers: molecular dynamics simulation studies. *In* Biological Membranes. K. Merz and B. Roux, editors. Birkhäuser, Boston.

Stouch, T. R., K. B. Ward, A. Altieri, and A. T. Hagler. 1991. Simulations of lipid crystals: characterization of the potential energy functions and parameters for lecithin molecules. *J. Computat. Chem.* 12:1033–1046.

Tieleman, D. P., and H. J. C. Berendsen. 1996. Molecular dynamics simulations of a fully hydrated dipalmitoylphosphatidylcholine bilayer with different macroscopic boundary conditions and parameters. *J. Chem. Phys.* 105(11):4871–4880.

Tu, K., D. J. Tobia, J. K. Blaise, and M. L. Klein 1996. Molecular dynamics investigation of the structure of a fully hydrated gel phase DPPC bilayer. *Biophys. J.* 70:595–608.

Van Buuren, A. R., and H. J. C. Berendsen. 1993. Molecular dynamics simulation of the stability of a 22-residue α-helix in water and 30% trifluoroethanol. *Biopolymers.* 33:1159–1166.

Vaz, W. L. C., and P. F. Almeida. 1991. Microscopic versus macroscopic diffusion in one-component fluid phase lipid bilayer membranes. *Biophys. J.* 60:1553–1554.

Venable, R. M., Y. Zhang, B. J. Hardy, and R. W. Pastor. 1993. MD simulations of a lipid bilayer and of hexadecane: an investigation of membrane fluidity. *Science.* 262:223–226.

Vogel, H., L. Nilsson, R. Rigler, K.-P. Voges, and G. Jung. 1988. Structural fluctuations of a helical polypeptide traversing a lipid bilayer. *Proc. Natl. Acad. Sci. USA.* 85:5067–5071.

Vogt, T. C. B., J. A. Killian, and B. de Kruijff. 1994. Structure and dynamics of the acyl chain of a transmembrane polypeptide. *Biochemistry.* 33:2063–2070.

Wiener, M. C., G. I. King, and S. H. White. 1991. Structure of a fluid dioleoylphosphatidylcholine bilayer determined by joint refinement of x-ray and neutron diffraction data. I. Scaling of neutron data and the distributions of double bonds and water. *Biophys. J.* 60:568–576.

Wiener, M. C., and S. H. White. 1991. Transbilayer distribution of bromine in fluid bilayers containing a specifically brominated analogue of dioleoylphosphatidylcholine. *Biochemistry.* 30:6997–7008.

Wiener, M. C., and S. H. White. 1992. Structure of a fluid dioleoylphosphatidylcholine bilayer determined by joint refinement of x-ray and neutron diffraction data. III. Complete structure. *Biophys. J.* 61: 434–447.

Weiss, M. S., and G. E. Schulz. 1992. Structure of porin refined at 1.8 angstroms resolution. *J. Mol. Biol.* 227:493.

White, S., and W. Wimley. 1994. Peptides in lipid bilayers: structural and thermodynamic basis for partitioning and folding. *Curr. Opin. Struct. Biol.* 4:79–86.

Wilson, M. A., and A. Pohorille. 1994. Molecular dynamics of a water-lipid interface. *J. Am. Chem. Soc.* 116:1490–1501.

Woolf, T. B., and B. Roux. 1996. Structure, energetics, and dynamics of lipid-protein interactions: a molecular dynamics study of the gramicidin A channel in a DMPC bilayer. *Protein Struct. Funct. Genet.* 24:92–114.

Xing, J., and H. L. Scott. 1989. Monte Carlo studies of lipid chains and gramicidin A in a model membrane. *Biochem. Biophys. Res. Commun.* 165:1–6.

Yeates, T. O., H. Komiya, A. Chirino, D. C. Ress, J. P. Allen, and G. Feher. 1988. Structure of the reaction center from *Rhodobacter sphaeroides* R-26 and 2.4.1: protein-cofactor (bacteriochlorophyll, bacteriopheophytin, and carotenoid) interactions. *Proc. Natl. Acad. Sci. USA.* 85:7993.

Yoon, D. Y., G. D. Smith, and T. Matsuda. 1993. A comparison of united atom and an explicit atom model in the simulation of polymethylene. *J. Chem. Phys.* 98:10037–10043.

Zhang, Y.-P., R. N. A. H. Lewis, G. D. Henry, B. D. Sykes, R. S. Hodges, and R. N. McElhaney. 1995a. Peptide models of helical hydrophobic transmembrane segments of membrane proteins. 1. Studies of the conformation, intrabilayer orientation, and amide hydrogen exchangeability of Ac-K2-(LA)12-K2-amide. *Biochemistry.* 34:2348–2361.

Zhang, Y.-P., R. N. A. H. Lewis, R. S. Hodges, and R. N. McElhaney. 1995b. Peptide models of helical hydrophobic transmembrane segments of membrane proteins. 2. Differential scanning calorimetric and FTIR spectroscopic studies of the interaction of Ac-K2-(LA)12-K2-amide with phosphatidylcholine bilayers. *Biochemistry.* 34:2362–2371.